HHS Public Access

Author manuscript

Bone. Author manuscript; available in PMC 2017 March 01.

Published in final edited form as:

Bone. 2016 March ; 84: 194–203. doi:10.1016/j.bone.2016.01.006.

Deficiency of Circadian Clock Protein BMAL1 in Mice Results in a Low Bone Mass Phenotype

William E. Samsa[a], **Amit Vasanji**[b], **Ronald J. Midura**[b], and **Roman V. Kondratov**[a]

William E. Samsa: samsa.william@gmail.com; Amit Vasanji: avasanji@image-iq.com; Ronald J. Midura: midurar@ccf.org

[a]Center for Gene Regulation in Health and Diseases, BGES, Cleveland State University, 2121 Euclid Ave., Cleveland, OH, 44115-2214

[b]Department of Biomedical Engineering, Cleveland Clinic, 9500 Euclid Ave., Cleveland, OH, 44195

Abstract

The circadian clock is an endogenous time keeping system that controls the physiology and behavior of many organisms. The transcription factor Brain and Muscle ARNT-like Protein 1 (BMAL1) is a component of the circadian clock and necessary for clock function. *Bmal1*$^{-/-}$ mice display accelerated aging and many accompanying age associated pathologies. Here, we report that mice deficient for BMAL1 have a low bone mass phenotype that is absent at birth and progressively worsens over their lifespan. Accelerated aging of these mice is associated with the formation of bony bridges occurring across the metaphysis to the epiphysis, resulting in shorter long bones. Using micro-computed tomography we show that *Bmal1*$^{-/-}$ mice have reductions in cortical and trabecular bone volume and other micro-structural parameters and a lower bone mineral density. Histology shows a deficiency of BMAL1 results in a reduced number of active osteoblasts and osteocytes *in vivo*. Isolation of bone marrow derived mesenchymal stem cells from *Bmal1*$^{-/-}$ mice demonstrate a reduced ability to differentiate into osteoblasts *in vitro*, which likely explains the observed reductions in osteoblasts and osteocytes, and may contribute to the observed osteopenia. Our data support the role of the circadian clock in the regulation of bone homeostasis and shows that BMAL1 deficiency results in a low bone mass phenotype.

Keywords

Biological clock; mesenchymal stem cell; aging; osteoblast; osteogenesis; bone

CORRESPONDING AUTHOR: Roman V. Kondratov, PhD, Center for Gene Regulation in Health and Disease, BGES, Cleveland State University, 2121 Euclid Ave., Science and Research Building, Cleveland, OH, 44115-2214, USA. Tel.: 216-523-7199; Fax: 216-687-6972; r.kondratov@csuohio.edu.

The authors declare no conflict of interest.

2.0 Introduction

Age-related deterioration of trabecular and cortical bone, coupled with disruption in normal mineral deposition and accumulation, causes alterations in bone architecture and a reduction in bone strength (Chen et al., 2013; Van der Linden et al., 2004). Bone remodeling requires strict control of two processes in which bone formation by osteoblasts and bone resorption by osteoclasts is necessary to maintain a healthy skeleton. Another bone cell, the osteocyte, is an important regulatory cell influencing and participating in bone remodeling through orchestrating both osteoblast and osteoclast activity (Schaffler et al., 2014). Importantly, osteocytes regulate mechanotransduction, as targeted ablation of osteocytes in mice results in increased cortical porosity and trabecular bone reduction, with resistance to unloading-induced bone loss (Tatsumi et al., 2007). Thus, osteocytes are a third bone cell necessary for maintenance of the structural integrity of bone. Several signaling pathways are implicated in the regulation of bone homeostasis and the circadian clock is one of these systems (Soltanoff et al., 2009; Fu et al., 2005). Over a quarter of murine calvarial bone genes are expressed with 24-hour periodicity (Zvonic et al., 2007). Additionally, there is a high bone mass phenotype present in mice lacking *Cry* or *Per* because of a dysregulation of leptin, through sympathetic nervous system signaling, ultimately controlling bone formation mediated by circadian clock signaling (Fu et al., 2005). Furthermore, genes involved in osteoblast differentiation are under circadian control; indeed, genes involved in mesenchymal stem cell differentiation and mineral deposition occur in a circadian fashion and are under direct control of the BMAL1:CLOCK complex (Zvonic et al., 2007; McElderry et al., 2013; Guntur et al., 2011; Dudek et al., 2014).

The circadian clock is an endogenous system present in most organisms that synchronizes their physiology and behavior with the earth's rotation (Buhr and Takahashi, 2013). It was previously shown that clock genes play a role in bone remodeling (Maronde et al., 2010; Fu et al., 2005). Using the *Per1,2*$^{-/-}$ double knockout mouse model of circadian disruption, Fu et al. demonstrated that the circadian clock is involved in leptin dependent regulation of osteoblast proliferation, and that the absence of the clock resulted in increased proliferation and bone formation (Fu et al., 2005). At the same time, it was reported that shift work (circadian disruption) results in lower bone mineral density and increases the risk of osteoporosis in humans (Freskanich et al., 2009; Quevedo & Zuniga, 2010). Therefore, these lines of evidence are seemingly at odds and suggest the connection between the circadian clock and bone homeostasis is more complicated than first thought arguing for the need of additional study. BMAL1 is a transcriptional factor playing a key role in the circadian clock mechanisms, and mice deficient in BMAL1 display an accelerated aging phenotype associated with non-orthotropic ossifications and lower bone weights often observed with older age (Kondratov et al., 2006a; Bunger et al., 2005). However, a definitive role of BMAL1 in regulating bone formation over an organism's lifespan is as yet undetermined.

Therefore, we hypothesized that BMAL1 is involved in the regulation of osteoblast differentiation and bone deposition, and decided to examine the bone phenotype of *Bmal1*$^{-/-}$ mice at varying ages and not just at an adolescent age (Fu et al., 2005). In this study, we used micro-computed tomography (micro-CT) scanning to show that BMAL1 deficiency in mice results in a low bone mass phenotype characterized by bone loss in both

cortical and trabecular bone compartments. Micro-CT scans of *Bmal1*$^{-/-}$ mouse long bones show lower bone volume fraction, decreased trabecular number and decreased cortical thickness compared to wild type littermates. Using conventional histomorphometry, we measured a lower number of active osteoblasts per bone surface and a significantly reduced number of osteocytes per bone area, the terminal differentiation product of osteoblasts, in *Bmal1*$^{-/-}$ mice as compared to wild type mice. Reductions in active osteoblast and osteocyte numbers likely contribute to the low bone mass phenotype. Follow up data revealed an impaired ability of bone marrow derived mesenchymal stem cells (MSCs) isolated from *Bmal1*$^{-/-}$ bone marrow to differentiate into osteoblasts in cell culture. This impaired osteogenic differentiation *in vitro* correlates with the reduced number of active osteoblasts and osteocytes *in vivo*. These *Bmal1*$^{-/-}$ mice data validate our hypothesis that the circadian clock is involved in age related bone homeostasis, and suggest another model of circadian disruption that may be used for studying bone homeostasis.

3.0 Experimental Procedures

3.1 Animals

Bmal1$^{-/-}$ mice were previously generated in Dr. C. Bradfield's laboratory (University of Wisconsin) (Bunger et al., 2000), and backcrossed to the C57BL/6J inbred strain (The Jackson Laboratory, Bar Harbor, ME, USA) for 12 generations. Wild type and knockout mice were generated by breeding of heterozygous parents. Genotypes were determined using a PCR-based method as previously described (Bunger et al., 2000). All animal studies were conducted in accordance with the regulations of the Committee on Animal Care and Use at Cleveland State University and Roswell Park Cancer Institute.

3.2 Micro-CT Imaging

Excised tibiae and femora scanned using GE eXplore Locus μCT (GE Healthcare, Piscataway, NJ) and 360 X-ray projections were collected in 1° increments (80 kVp; 500 μA; ~40 minute total scan time). Projection images were preprocessed and reconstructed into 3-dimensional volumes (1024^3 voxels, 20 μm resolution) on a 4PC reconstruction cluster using a modified tent-FDK cone-beam algorithm (GE reconstruction software). Three-dimensional data were processed and rendered (isosurface/maximum intensity projections) using MicroView (GE Healthcare). Tibial segmentation from surrounding bone, volume enhancement, and delineation of regions-of-interest (ROIs) were performed in MicroView. For the tibiae, a ROI extending from below the proximal tibial growth plate to the distal fibular/tibial synostosis was created and then subsequently split into 3 contiguous regions: 0–25%, 25–50%, and 50–100% of the total ROI length. ROI's were created using the same approach for femora with the initial ROI extending from above the distal femoral growth plate to immediately below the femoral neck. For both femora and tibiae, measurements were taken at a distance from the growth plate that excludes the primary spongiosa.

3.3 Dissection of Femora and Tibiae and Isolation of Marrow Stromal Cells

For the isolation of femora and tibiae for histological staining, young (4 week-old) and adult (24, 32 and 36 week-old) wild type and Bmal1$^{-/-}$ mice were euthanized by CO_2

asphyxiation followed by cervical dislocation. Skin was removed from the hind legs, soft tissues were dissected away with forceps and adherent nonosseous tissue was removed with surgical scissors. For isolation of marrow MSCs, femora and tibiae were disarticulated from 7–9 month old wild type and Bmal1$^{-/-}$ mice under aseptic conditions and the epiphyses were removed. Total bone marrow was flushed from tibiae and femora with 5 mL of α-MEM by inserting a 22-gauge syringe needle into the end. Cells from the marrow tissue were separated by fluid shear and plated for culture. Three days after plating media was replaced to remove non-adherent cells.

3.4 Cell Culture

All cells were maintained in Minimal Essential Medium α (α-MEM) (LRI, Cleveland Clinic, Cleveland, USA) supplemented with 10% Defined FBS (Atlanta Biologicals, USA) and 10000 units of Penicillin G and 10000 μg/ml streptomycin (LRI, Cleveland Clinic, Cleveland, USA). Cells were maintained under standard growth conditions at 37°C in a humidified atmosphere with 5 % CO_2. Media was replaced twice a week.

3.5 Decalcification and Histology

Femora were disarticulated from 6–7 month old wild type and 5–6 month old Bmal1$^{-/-}$ mice and following the removal of soft tissue, decalcified and fixed in a 1:20 tissue:fixative volume ratio of Cal-Rite (Thermo Scientific) for 14 days, with Cal-Rite being replaced every 24 hours. All samples were paraffin embedded using the Leica TP1020 tissue processor, after serial dehydration with a graded series of ethanol washes to Clear-Rite (Thermo Scientific). All bones were oriented in such a manner that cuts were made yielding a medial to lateral presentation. Tissue sections (10 μm thick) were cut and placed onto gelatin-coated Superfrost+ slides, and then stained with hematoxylin and eosin. The aspect ratio of a cell (and its nucleus) was used to determine if osteoblasts were active, partially active or inactive as described previously (Pritchard 1972). Briefly, images were analyzed in ImageJ to determine the number and aspect ratio of osteoblasts present on the surface of the periosteal bone, endosteal bone, and the trabecular compartment. Total number of osteoblasts, as well as the number of osteoblasts categorized into active, partially active and inactive were normalized to the length of bone surface in ImageJ and quantified as number of cells per millimeter. Using ImageJ, aspect ratio was determined and an aspect ratio of 1:1 to 1:4 were marked as active, 1:5 to 1:9 were marked as partially active, and 1:10 or greater were marked as inactive, as demonstrated in Supplementary Figure 2.

3.6 Osteoblast Differentiation In vitro

For osteogenic differentiation, adherent cells were sub-cultured 3 times and plated into 96 well plates at 2.0×10^3 cells per well. Cells were cultured for 0, 14 and 21 days in either control or differentiation media followed by alizarin red staining. For colony forming unit assay, total bone marrow was flushed and plated directly into 6 well plates at 2.0×10^6 cells per well. After 72 hours, non-adherent cells were removed by replacing media with either fresh media or differentiation media. These primary cell cultures were incubated for 18 days at which time they fixed and stained by alizarin red S, von Kossa, alkaline phosphatase and crystal violet staining procedures.

3.7 Staining and Colony Counting

Mineralization of osteoblasts was determined using Alizarin Red S Staining (ARS) and von Kossa Staining (VK). For ARS, cells were washed twice in ice cold Hank's Balanced Salt Solution (HBSS) and fixed in ice cold 70% ethanol/1mM Hepes pH 7.0 overnight at 4°C. Cells were washed twice with 1mM Hepes pH 7.0 and stained with 4mM ARS at pH 4.2 for 10 min at room temperature (Stanford et al., 1995). Cells were then washed 3 times in 1mM Hepes pH 7.0. For VK, cells were washed twice with ice cold HBSS and fixed for 30 min in 10% neutral buffered formalin. Cultures were rinsed twice with distilled water and incubated in the dark for 10 min in 2% silver nitrate. Cells were rinsed 3 times with distilled water and exposed to light for 15 min. Cells were dehydrated in 100% ethanol and air dried for image analysis. For Alkaline Phosphatase Staining, cultures were rinsed twice with HBSS, fixed for 30s in citrate buffered acetone, washed with distilled water, and stained in the dark for 45 min at room temperature with Naphthol AS-MX in fast violet. Cultures were then rinsed twice with distilled water and air dried for image analysis. For crystal violet staining (CV), cultures were rinsed twice with phosphate-buffered saline (PBS), fixed in 10% neutral buffered formalin, and followed by staining with 0.05% CV for 30 min. Cells were washed with distilled water and air dried for image analysis. ARS, VK and ALP colony counting was done by 3 independent investigators blinded to experimental conditions. For ARS quantification, stained cultures were incubated in ice cold 10mM HCl/70% ethanol and rotated for 15 minutes (Wang et al. 2000). Extract was transferred to a tube followed by a second incubation which was transfered to its corresponding tube. Absorbance was then measured at 405nm.

3.8 Statistical Analysis

All results are presented as a mean ± standard deviation. Statistical significance was determined using a 1 tailed unpaired Students' t test.

4.0 Results

4.1 BMAL1 deficiency results in the formation of bridges of bone spanning the epiphyseal growth plate

We conducted a gross examination of long bones isolated from male wild type and *Bmal1*$^{-/-}$ mice and found a significant reduction in the length of femora and tibiae in *Bmal1*$^{-/-}$ mice as compared to wild type mice at 9 months of age (Fig 1A). As both genders display age associated loss of bone mass, males were exclusively used in order to control for any effects that may result from estrogen deficiency at menopause. Micro-CT measurements of bone length confirmed a significant decrease in the length of long bones in BMAL1 deficient mice when compared to age-matched wild type littermates (Fig 1B), as did caliper measurements (data not shown).

Longitudinal bone growth occurs at the epiphyseal growth plate as a result of expansion and calcification of the cartilage layer. At 4 weeks of age, histological staining does not show any noticeable difference in the thickness of the epiphyseal growth plate in mice of both genotypes. At 32 weeks of age there is an apparent reduction in the thickness of the epiphyseal growth plate in both *Bmal1*$^{-/-}$ and wild type mice, but this age-dependent

reduction appears relatively greater in knockout mice. We also observed that at 8 months of age *Bmal1*$^{-/-}$ mice exhibited bridges of bone spanning the growth plate cartilage boundaries (indicated inside the black box in Fig. 1C), indicating that fusion of the epiphysis and metaphysis has occurred (i.e., cessation of longitudinal growth and epiphyseal growth plate bridging). Substantiating these histological findings, micro-CT scanning confirmed that an open epiphyseal growth plate is still present in wild type mice at 36 weeks of age, whereas in *Bmal1*$^{-/-}$ mice, the growth plate appears closed at 24 weeks of age (Fig 1C, white arrows). Our finding that long bones in skeletally mature *Bmal1*$^{-/-}$ mice are reduced in length compared to wild type littermates extend upon those reported by Takarada et al. (2012) for 1 month old juvenile *Bmal1*$^{-/-}$ mice. Our data suggest that this shortening in bone length is a result of a relatively greater age-dependent thinning of the growth plate cartilage and the appearance of bone tissue bridges that form across the epiphyseal growth plate at an earlier age.

4.2 BMAL1 deficiency results in altered trabecular and cortical bone morphology and reduced bone mineral density (BMD)

Age related decreases in bone mass are often associated with alterations in trabecular and cortical bone microstructure (Halloran et al., 2002). We investigated bone architecture using micro-CT scanning of femora and tibiae from adolescent (8 week old) and skeletally mature adult (7–9 month old) wild type and *Bmal1*$^{-/-}$ mice. Figure 2A shows a 3D rendering of the region of interest from the proximal tibia that was used for trabecular bone measurements. Trabecular bone morphology of femora and tibiae differ consistently with age for both genotypes, and the age-related changes in the bone architecture of wild type mice is similar to those reported by others, with the volume of trabecular bone being higher during juvenile growth as compared to adulthood (Tables S1 and S2)(Ferguson et al., 2003).

The micro-CT data shown represents the region of interest in femora and tibiae that extends from 0–25% below the growth plate, as described in experimental procedures. Figure 2A highlights the ROI examined extending from below the growth plate and excluding the primary spongiosa, as per convention (Bouxsein et al., 2010). Similar results were obtained in regions extending 25–50% and 50–100% from this region of interest, indicating that these bone parameters exist throughout the entire length of long bones. In *Bmal1*$^{-/-}$ mice, we observed a reduction in trabecular bone volume fraction (BV/TV) compared with wild type mice (Fig. 2B and 2C). In young mice there was a significant, 32% decrease in femora, and in tibiae we observed a trend towards reduction. In adult mice the reduction in BV/TV was detected in both femora (59%) and tibiae (44%). There is a significant decrease in trabecular number in the femora of *Bmal1*$^{-/-}$ mice compared to wild type mice, with young BMAL1 deficient mice having a 26% reduction, which worsens to a 63% reduction by an adult age (Figure 2B, middle panel). In tibiae, a significant decrease of 52% in the trabecular number of knockouts was noted at a young age and a trend towards a reduction at an adult age (Figure 2C, middle panel). Furthermore, we observed no significant difference in trabecular thickness, except for an 8% reduction in the adult *Bmal1*−/− tibia, which corroborates others' work (Halloran et al., 2002). Therefore, a significant reduction in trabecular bone volume fraction in both the femora and tibiae of *Bmal1*$^{-/-}$ mice compared to wild type mice exists, with the reduction in femora resulting from a decrease in trabecular number at both

ages, and the reduction in adult tibiae resulting from a reduction from a modest thinning of trabeculae. Cortical bone parameters were also observed to be decreased in *Bmal1*$^{-/-}$ mice when compared to wild type mice. Cortical bone thickness was significantly reduced in both the femora and tibiae of *Bmal1*$^{-/-}$ mice at both age groups (Fig. 3), which contributes to the reduction in bone volume fraction observed in BMAL1 deficient mice (Tables S3 and S4). Similar results were obtained throughout the diaphysis, showing that the cortical thickness was reduced at the mid-shaft too. Therefore, both cortical and trabecular bone mass homeostasis has been significantly affected by BMAL1 deficiency and these datasets lead us to the conclusion that BMAL1 deficient mice exhibit a low bone mass phenotype.

An increase in trabecular and cortical BMD occurs from young to adult-aged bone, and as expected, we observe this in both femora and tibiae of wild type mice. We also observe this trend in BMAL1 deficient mice (Fig. 4A and 4B; Tables S1 and S4) (Ferguson et al., 2003). There is a significant decrease in *Bmal1*$^{-/-}$ mice of trabecular and cortical BMD in both femora (Figure 4A) and tibiae (Figure 4B) when compared to wild type mice. Thus, while we observe age-related changes in bone microstructure and BMD occurring in both wild type and *Bmal1*$^{-/-}$ mice, we note reductions in these parameters in BMAL1 deficient mice as compared to wild type mice. Accordingly, we conclude that the low bone mass phenotype observed in BMAL1 deficient mice is a result of a decrease in trabecular parameters and cortical bone thickness, as well as a reduction in the bone mineral density.

4.3 Bmal1$^{-/-}$ mice display a reduced number of osteoblasts and osteocytes

One possible mechanism for the reduction in bone mass could be that there is a reduced number of bone forming osteoblasts in *Bmal1*$^{-/-}$ mice. In order to determine if there was a reduced number of osteoblasts per bone surface, we conducted H&E staining of longitudinal sections at the midline of femora isolated from adult wild type (6–7 month old) and BMAL1 deficient (5–6 month old) mice (Figure 5). The chosen ages of mice reflect that by 5 month of age, C57BL/6 mice are skeletally mature, have reached peak bone mass, and little change occurs in bone mass from 6–12 months of age (Brodt et al., 1999; Jilka 2013). As our Micro-CT data showed different alterations in bone mass in the trabecular and cortical compartments of bone, we calculated the number of osteoblasts present at the endosteum and periosteum of cortical bone, as well as those along the trabecular bone surfaces (Figure 5A). We further categorized the osteoblasts into three types (active, partially active, and inactive) depending on the morphology of the cell in order to better understand what bone forming activities were occurring in each bone region (Figure 5C)(Pritchard 1972; Pritchard 1952).

Figure 5A shows the results of counting osteoblasts on the endosteal surface (left panel). There is a small, non-significant decrease in the total number of osteoblasts per bone surface in BMAL1 deficient mice compared to wild type mice. Interestingly, when this cell population was scored for histological appearance of an active state, we noted non-significant decreases in the number of active and partially active osteoblasts, and a significant increase in the number of inactive osteoblasts, with *Bmal1−/− mice having a 3.2 fold increase in the number of inactive osteoblasts compared to wild type*. This indicates that while total osteoblast number at the endosteal surface is relatively unchanged, there is a

decreased overall activity of osteoblasts along this bone surface. On the periosteal surface, there exists again a slight, non-significant decrease in the total number of osteoblasts. Unlike the endosteal surface, the periosteal surface revealed significant changes in osteoblast activity, with an 80% decrease in the number of active osteoblasts, a 50% decrease in the number of partially active osteoblasts, and a 32% increase in the number of inactive osteoblasts per bone surface in *Bmal1*$^{-/-}$ mice compared to wild type mice. This indicates that along the cortical surfaces of BMAL1 deficient mice the lowered bone mass correlates with a reduction in active osteoblasts and an increase in the number of inactive osteoblasts. In trabecular bone, there is a slight, non-significant decrease in the total number of osteoblasts, and non-significant changes in the number of inactive osteoblasts in *Bmal1*$^{-/-}$ mice. However, a significant reduction in the number of active osteoblasts per bone surface was measured in BMAL1 deficient mice compared to wild type mice, as shown by a 72% reduction. These data show that there is a reduced number of active osteoblasts and an increased number of inactive osteoblasts *in vivo* in BMAL1 deficient mice compared to wild type mice, suggesting decreased osteogenic activities as a mechanism to explain the reduced cortical and trabecular bone parameters in these mice.

Osteocytes are important regulators of bone homeostasis; they orchestrate osteoblast and osteoclast activity in response to mechanical stimulation (Shaffler et a., 2014; Bellido 2014; Franz-Odendaal et al., 2006). We observed a significant 22% decrease in total osteocyte lacunar number in the bones of *Bmal1*$^{-/-}$ mice, on average 1098 osteocytes per mm^2 for wild type and 852 osteocytes per mm^2 for *Bmal1*$^{-/-}$ mice (Figure 5B and lower panels of 5C). In addition to a decreased density of lacunae in the bones of *Bmal1*$^{-/-}$ mice, we also noticed a difference in the lacunar content and the morphology of osteocytes within the lacunae. In wild type mice, lacunae were very prevalent, and contain generally round/ovoid and spherical osteocytes nearly filling the lacunae, whereas in *Bmal1*$^{-/-}$ mice, the number of lacunae was less, the cell volume was decreased in relation to the lacunae area, and the cells were irregularly shaped (Figure 5C, lower panels). A significant decrease in the number of osteocytes per bone area in BMAL1 deficient mice as compared to wild type mice indicates a deficiency in osteoblast terminal differentiation. This finding is consistent with our hypothesis that decreased osteogenic activities are a mechanism to explain the reduced cortical and trabecular bone parameters in BMAL1 deficient mice.

4.4 Impairment of osteoblast differentiation in BMAL1 deficient mice

Osteoblasts associated with trabecular bone and the endo-cortical surface are derived from mesenchymal stem cells (MSCs) residing in bone marrow. In order to determine the osteogenic potential of *Bmal1*$^{-/-}$ MSCs, we conducted *in vitro* differentiation assays with primary and passaged cultures of bone marrow stromal cells. Figure 6A shows the results of *in vitro* osteoblast differentiation of passaged bone marrow MSCs from wild type and *Bmal1*$^{-/-}$ mice. Bone marrow MSCs were isolated from femora and tibiae of wild type and *Bmal1*$^{-/-}$ mice, and cells were passaged 3 times followed by plating into 96 well plates and cultured in normal growth media or osteogenic differentiation media. Mineralization (the functional endpoint of osteoblast differentiation) was assayed by staining with a calcium mineral binding dye, alizarin red S (ARS), at 0, 14 and 21 days after switching to differentiation media (Wang et al., 2000). BMAL1 deficient cells demonstrated a reduction

in the onset time and amount of mineralization as compared to wild type MSCs as shown in culture and by quantification of Alizarin Red stain (Figure 6A). These data demonstrate a reduced *in vitro* mineralization of bone marrow derived osteoprogenitor cells and are in agreement with the reduced number of active osteoblasts and osteocytes in *Bmal1*$^{-/-}$ mice. Altogether, these datasets may help to explain the low bone mass phenotype of *Bmal1*$^{-/-}$ mice.

The reduced ability of *Bmal1*$^{-/-}$ cells to differentiate into functional osteoblasts can be explained in two different ways. First, there may be impairment in the ability of MSCs isolated from *Bmal1*$^{-/-}$ mice to differentiate, or second, there can be a fewer number of stem/progenitor cells in the bone marrow of these mice. First we determined if there is a difference in number of stem/progenitor cells in *Bmal1*$^{-/-}$ mice. We plated 2 million nucleated cells per 60 mm dish, and after three weeks we stained the plates with crystal violet. We found that (when cultured in regular growth media) the number of crystal violet-stained colony forming units (CFUs) were similar for both wild type and *Bmal1*$^{-/-}$ bone marrow (15 ± 10 for wild type cells and 13 ± 10 for Bmal1$^{-/-}$ cells). However, when cultured under osteogenic differentiation conditions we observed a non-significant decrease in the number of CFUs that formed in isolated *Bmal1*$^{-/-}$ bone marrow stromal cells compared to wild type; wild type showed an average of 17 ± 8 CFUs and BMAL1 deficient showed 14 ± 7 CFUs. CFUs were also stained for mineralization using two different staining procedures (ARS for calcium and von Kossa, VK, for phosphate) as well as for alkaline phosphatase (ALP) activity, a known early marker of osteogenic differentiation. *Bmal1*$^{-/-}$ marrow derived MSCs showed a reduction in the number of CFUs that stained positive for mineral: ARS staining shows 76% positive CFUs in wild type and 40% in *Bmal1*$^{-/-}$; VK staining shows 75% positive CFUs in wild type and 43% in BMAL1 deficient CFUs. Nearly all wild type CFUs stained positively for ALP, compared to only 57% of *Bmal1*$^{-/-}$ CFUs (Figure 6B). These data indicate that there is reduced number of osteoprogenitors or a reduced ability to differentiate into osteprogenitors in BMAL1 deficient bone marrow MSCs. There was also a noticeable reduction in the size of the colonies and the intensity of staining for all three stains, indicating that there may be other defects in the early and late stages of differentiation in *Bmal1*$^{-/-}$ osteoprogenitors, further confirming the reduced osteogenic potential of *Bmal1*$^{-/-}$ bone marrow MSCs.

5.0 Discussion

We found that for both trabecular and cortical bone tissues, BMAL1 deficiency resulted in the development of a low bone mass phenotype in both young and older mice. First, BMAL1 deficient mice display an earlier closure of growth plates than wild type mice, even though it is known that murine growth plates do not exhibit clear signs of closure by 12 months of age (Vogel et al., 1999; Jilka et al., 2013). The reduced thickness of *Bmal1*$^{-/-}$ growth plates would also suggest alterations in endochondral bone formation. Indeed, it was recently reported that clock genes, and *Bmal1* in particular, are involved in cartilage homeostasis (Takarada et al., 2012). In this study, the authors show that circadian rhythms in gene expression exist for clock genes and the master regulator gene of chondrogenesis, *Indian Hedgehog*, in the rib growth plate and chondrocyte differentiation is negatively affected by BMAL1 deficiency. The experiments were performed in one day old mice and

address the role of BMAL1 and circadian rhythms in embryonic and post natal bone formation. Our data extends these observations and address the role of BMAL1 in epiphyseal growth plate homeostasis during bone growth in young (4 weeks of age) and adult (32 weeks of age) mice. We did not find any significant difference in the growth plate morphology for young mice and found abnormal bony bridge formation across the hyaline cartilage layer of the epiphyseal growth plate in *Bmal1*$^{-/-}$ mice. Formation of bony bridges is unusual for mice, which suggests that BMAL1 is essential for normal physiology of the epiphyseal growth plate. Our investigation also corroborated previous studies showing ectopic calcification and arthropathies in the diarthrotic joints of BMAL1 deficient mice; micro-CT data showed ectopic soft tissue mineralization and osteophyte-like projections present on long bone surfaces (Figure S1) (Bunger et al., 2005).

We also found that in both femora and tibiae of adults, BMAL1 deficiency results in a 30% reduction in BMD by 7 months of age. This striking drop in BMD is remarkable, as even a 10% decrease in BMD in humans has been calculated to roughly double the risk of fracture (Keaveny & Hayes 1993). The reduction in BMD of *Bmal1*$^{-/-}$ long bones, coupled with the reduction in cortical thickness, should result in an inferior bending strength and reduction in the ability to withstand mechanical loading when compared to wild type bones. Indeed, preliminary cantilever bend testing shows an inferior bending strength in adult *Bmal1*$^{-/-}$ long bones compared to wild type animals (data not shown), and we observed a higher incidence of inadvertent fracture during surgical recovery of *Bmal1*$^{-/-}$ long bones.

Bone loss is associated with an uncoupling of formation and resorption during the bone remodeling process (O'Brien et al., 2013). During bone remodeling, inferior bone tissue is resorbed by osteoclasts, which then signal osteoprogenitors and osteoblasts to repair and refill the excavated site with new bone tissue. It was previously shown that osteoclast activity as measured by urinary elimination of deoxypyridinoline, a collagen breakdown product and marker of osteoclast activity, was not different between wild type and circadian mutant mice (Fu et al., 2005). While we cannot completely exclude the possibility that bone resorption is also affected in BMAL1 deficient mice, and future studies are needed to answer if BMAL1 or other clock proteins play any role in osteoclast physiology, here we provide definitive evidence that a deficiency of BMAL1 results in impaired osteoblast differentiation *in vitro*, which correlates with a reduced number of functional osteoblasts and osteocytes *in vivo*. Our findings recapitulate those of models of accelerated aging, including the *wrn*$^{-/-}$ terc$^{-/-}$ mouse model and the *ku86* knock out mouse, which results in accelerated aging senile osteoporosis, and reduced lifespan (Vogel et al., 1999; Pignolo et al., 2008).

The decrease in the number of osteocytes in *Bmal1*$^{-/-}$ mice is particularly striking. Osteocytes are the most numerous cells in bone, composing up to 95% of all bone cells, and can live for decades in long-living animals (Shaffler et al., 2014; Bellido 2014) Osteocytes are responsible for regulating bone remodeling through the sensing of mechanical strain; therefore, the large decrease in osteocyte number in *Bmal1*−/− mice not only shows a decrease in terminal differentiation of osteoblasts, but also suggests a plausible mechanism for a decrease in bone formation (Tatsumi et al., 2007). However, further experiments are needed to establish this mechanism as a reduction in osteocytes may also be a result of increased apoptosis or other type of cell death. As such, osteocyte apoptosis is associated

with increased bone resorption, low bone accrual and defects in mechanical response to weightlessness (Bellido 2014; Emerton et al., 2010; Maurel et al., 2011; Tatsumi et al., 2007). Regardless, normal aging in humans and mice, as well as progeria phenotypes in murine mutant strains are known to exhibit skeletal fragility as a result of reduced osteoblast numbers (Jilka 2012; Almeida 2012).

Our study further connects the circadian clock to the regulation of bone homeostasis. It was previously reported that mineral deposition occurs with an approximately 24-hr periodicity (Zvonic et al., 2007; McElderry et al., 2013; Meyer et al., 2000), Period 2 (Okobu et al., 2013) and Runx2 (Reale et al., 2013) are rhythmically expressed in bone. Finally, the disruption of core circadian clock genes affects bone phenotypes in mice (Fu et al., 2005; Maronde et al., 2010; Meyer et al., 2000). The circadian clock is involved in systemic control of bone remodeling, which occurs through a sympathetic nervous system hypothalamic relay mediated by leptin (Fu et al., 2005). The authors proposed that the circadian clock mediates the anti-proliferative function of sympathetic signaling by inhibiting osteoblast proliferation. In agreement with that, mice with a double knockout for circadian clock genes *Periods* 1 and 2 or double knockout for circadian clock genes *Cryptochromes* 1 and 2 have an increased bone deposition rate and a high bone mass phenotype. The central conclusion from the study was that circadian disruption leads to increased osteoblast proliferation and increased bone formation. In the same study, Fu and colleagues also report increased mineral apposition rate and osteoblast number in young *Bmal1*$^{-/-}$ mice. Our study suggests that the interaction between the circadian clock and bone homeostasis is more complicated. Indeed, we report here that *Bmal1*$^{-/-}$ mice have a low bone mass phenotype, a reduced number of active osteoblasts and mature osteocytes *in vivo*, and decreased osteoblast differentiation in vitro. The principal difference between ours and the cited study is that Fu and colleagues performed most of the experiments on 2 month old mice, which is before the skeleton has reached peak bone mass; or in other words, when bone accrual and longitudinal bone growth is still occurring (Jilka et al., 2012), while in our study, most of the experiments were performed on mice older than 5 months of age. Therefore, our study is an extension to the previous reports on the role of the circadian clock in bone physiology. Indeed, previous studies address the role of the clock in developing bones, while our study demonstrated that clock protein BMAL1 is essential for mature bone homeostasis in vivo. In addition our data suggest that the circadian clock is also involved in cell (osteoblast) autonomous mechanisms.

There are several possible explanations as to why circadian disruption through PERs and CRYs, as shown by Fu et al., has an opposite effect on bone formation than BMAL1 deficiency. First, PERs and CRYs represent the negative arm of the circadian feedback loop, and BMAL1 is a positive arm element, therefore deficiency of positive and negative elements of the molecular clock may have different effects on the control of clock gene expression. Second, increased bone formation has been observed in young *Cry* and *Per* deficient mice, which does not display premature aging, while reduced bone volume fraction has been observed in older *Bmal1*$^{-/-}$ mice. Thus, the circadian clock may have a different influence on bone formation in young versus old organisms. Third, circadian clock proteins have circadian clock independent functions and the bone phenotype observed in BMAL1

deficient mice may be unique to BMAL1 deficiency rather than for clock disruption. In agreement with our observation, it has been reported that circadian mineral deposition in calvaria correlates with BMAL1 transcriptional activity (McElderry et al., 2013).

We propose the following mechanisms of low bone mass in BMAL1 deficient mice: circadian clocks are involved in systemic and osteoblast specific control of bone formation, and circadian disruption will affect both levels of control. Disruption of the *Period* genes results in a high bone mass due increased osteoblast proliferation in a systemic manner acting through the molecular clock in osteoblasts, whereas disruption of *Bmal1* results in a low bone mass in a call autonomous manner resulting from a depletion of osteoprogenitors and their reduced ability to differentiate into osteoblasts and deposit bone matrix. This model is supported by recent observations that the reduced capacity of marrow stromal cells from aged mice to proliferate correlates with decreased mRNA and protein levels of BMAL1, while BMAL1 deficiency results in an increase in the number of senescent cells in different tissues, including bone marrow stromal cells (Chen et al., 2012; Lin et al., 2013; Khapre et al., 2011; He et al., 2013). Further experiments using conditional, tissue specific knock outs are needed to dissect systemic and cell autonomous mechanisms of the circadian clock and BMAL1 dependent control of bone formation.

In summary, BMAL1 plays a functional role in regulating bone homeostasis through control of mesenchymal stem cell differentiation into mature osteoblasts *in vitro* and BMAL1 deficiency results in a low bone mass phenotype *in vivo*. Our study raises several important questions: one of them is what is the molecular mechanism of BMAL1 dependent control of osteoblast differentiation? BMAL1 is a transcriptional factor and may regulate the expression of genes important for osteoblast differentiation. BMAL1 also controls oxidative stress response (Patel et al., 2014), the mTOR signaling pathway (Jouffe et al., 2013; Khapre et al., 2014) and translation (Lipton et al., 2015), which can contribute to osteoblast differentiation. Future studies are needed to answer these questions. Degeneration of bone with aging is a complex phenomenon, with a decrease in bone quality and quantity being affected by biochemical signaling in paracrine, autocrine and systemic manners. The complexity of bone remodeling is further highlighted by how changes in these facets of regulation occur in response to environmental stimuli such as diet and mechanical loading (Riddle et al., 2014; Boccafoschi et al., 2013). As the circadian clock regulates many aspects of physiology, dissecting exact mechanisms requires further investigation. Our results provide a link between the circadian clocks and bone mass homeostasis, with BMAL1 having some cell autonomous effects on bone formation, and establish *Bmal1*$^{-/-}$ mice as a model to study bone homeostasis.

Supplementary Material

Refer to Web version on PubMed Central for supplementary material.

Acknowledgments

The authors also thank Dr. Caroline Androjna and Sharon Midura for their instructions on how to isolate and culture marrow stromal cells from long bone marrow, help with image processing and preliminary cantilever bend

testing. This research was supported by R01 AG039547 and Funds from GRHD center to R.V.K and the Dissertation Research Award from Cleveland State University to W.E.S.

The abbreviations used are

BMAL1	Brain and Muscle ARNT-Like Protein 1
MSCs	Mesenchymal Stem Cells
CLOCK	Circadian Locomotor Outpur Cycles Kaput
Per1	Period 1
Per2	Period 2
Cry1	Cryptochrome 1
Cry2	Cryptochrome 2
Rev-Erb α	Nuclear Receptor Subfamily 1, Group D, Member 1
CCGs	Clock Controlled Genes
Micro-CT	Micro Computed Tomography
ROI	Region of Interest
Tb.Th.	Trabecular Thickness
Tb.N.	Trabecular Number
BV/TV	Bon Volume per Tissue Volume
BMD	Bone Mineral Density
BMC	Bone Mineral Content
ARS	Alizarin Red S
VK	Von Kossa
ALP	Alkaline Phosphatase
CV	Crystal Violet
HBSS	Hank’s Balanced Salt Solution

References

1. Almeida M. Aging mechanisms in bone. Bonekey Rep. 2012 Jul 1.:1. pii 102. [PubMed: 23951413]
2. Bellido T. Osteocyte-driven bone remodeling. Calcif. Tissue Int. 2014 Jan; 94(1):25–34. [PubMed: 24002178]
3. Boccafoschi F, Mosca C, Ramella M, Valente G, Cannas M. The effect of mechanical strain on soft (cardiovascular) and hard (bone) tissues: common pathways for different biological outcomes. Cell Adh. Migr. 2013; 7(2):165–173. [PubMed: 23287581]
4. Bouxsein ML, Boyd SK, Christiansen BA, Guldberg RE, Jepsen KJ, Müller R. Guidelines for the assessment of bone microstructure in rodents using micro-computed tomography. J. Bone Miner. Res. 2010 Jul; 25(7):1468–1486. [PubMed: 20533309]
5. Brodt MD, Ellis CB, Silva MJ. Growing C57Bl/6 mice increase whole bone mechanical properties by increasing geometric and material properties. J. Bone Miner. Res. 1999 Dec; 14(12):2159–2166. [PubMed: 10620076]

6. Buhr ED, Takahashi JS. Molecular components of the Mammalian circadian clock. Hanb. Exp. Pharmacol. 2013; 217:3–27.
7. Bunger MK, Walisser JA, Sullivan R, Manley PA, Moran SM, Kalscheur VL, Colman RJ, Bradfield CA. Progressive Arthopathy in mice with a targeted disruption of the Mop3/Bmal-1 locus. Genesis. 2005 Mar; 41(3):122–132. [PubMed: 15739187]
8. Bunger MK, Wilsbacher LD, Moran SM, Clendenin C, Radcliffe LA, Hogenesch JB, Simon MC, Takahashi JS, Bradfield CA. Mop3 is an essential component of the master circadian pacemaker in mammals. Cell. 2000 Dec 22; 103(7):1009–1017. [PubMed: 11163178]
9. Chen H, Zhou X, Fujita H, Onozuka M, Kubo KY. Age-related changes in trabecular and cortical bone microstructure. Int. J. Endocrinol. 2013; 2013:213–234.
10. Chen Y, Xu X, Tan Z, Ye C, Zhao Q, Chen Y. Age-related BMAL1 change affects mouse bone marrow stromal cell proliferation and osteo-differentiation potential. Arch. Med. Sci. 2012 Feb 29; 8(1):30–38. [PubMed: 22457671]
11. Dudek M, Meng QJ. Running on time: the role of circadian clocks in the musculoskeletal system. Biochem. J. 2014 Oct 1; 463(1):1–8. [PubMed: 25195734]
12. Emerton KB, Hu B, Woo AA, Sinofsky A, Hernandez C, Majeska RJ, Jepsen KJ, Shaffler MB. Osteocyte apoptosis and control of bone resorption following ovariectomy in mice. Bone. 2010 Mar; 46(3):577–583. [PubMed: 19925896]
13. Ferguson VL, Ayers RA, Bateman TA, Simske SJ. Bone development and age-related bone loss in male C57BL/6J mice. Bone. 2003 Sep; 33(3):387–398. [PubMed: 13678781]
14. Franz-Odendaal TA, Hall BK, Witten PE. Buried alive: how osteoblasts become osteocytes. Dev. Dyn. 2006 Jan; l235(1):176–190. [PubMed: 16258960]
15. Freskanich D, Hankinson SE, Schernhammer ES. Nightshift work and fracture risk: the Nurses' Health Study. Osteoporos Int. 2009 Apr; 20(4):537–542. Epub 2008 Sep 3. [PubMed: 18766292]
16. Fu L, Patel MS, Bradley A, Wagner EF, Karsenty G. The molecular clock mediates leptin-regulated bone formation. Cell. 2005; 122(5):803–815. [PubMed: 16143109]
17. Guntur AR, Kawai M, Le P, Bouxsein ML, Bornstein S, Green CB, Rosen CJ. An essential role for the circadian-regulated gene nocturnin in osteogenesis: the importance of local timekeeping in skeletal homeostasis. Ann N Y Acad Sci. 2011 Nov.1237:58–63. [PubMed: 22082366]
18. Halloran BP, Ferguson VL, Simske SJ, Burghardt A, Venton LL, Majumdar S. Changes in bone structure and mass with advancing age in the male C57BL/6J mouse. J. Bone Miner. Res. 2002 Jun; 17(6):1044–1050. [PubMed: 12054159]
19. He Y, Chen Y, Zhao Q, Tan Z. Roles of Brain and muscle ARNT-like 1 and Wnt antagonist Dkk1 during osteogenesis of bone marrow stromal cells. Cell Proliferation. 2013; 46(6):644–653. [PubMed: 24460718]
20. Jilka RL. The relevance of mouse models for investigating age-related bone loss in humans. J. Gerontol. A. boil. Sci. Med. Sci. 2012 Oct; 68(10):1209–1217. Epub 2013 May 20.
21. Jouffe C, Cretenet G, Symul L, Martin E, Atger F, Naef F, Gachon F. The circadian clock coordinates ribosome biogenesis. PLoS Biol. 2013; 11(1):e1001455. [PubMed: 23300384]
22. Keaveny, TM.; Hayes, WC. Mechanical properties of cortical and trabecular bone. In: Hall, BK., editor. bone. Vol. 7. Boca Raton, FL: CRC Press; 1993. p. 285-344.
23. Khapre RV, Kondratova AA, Susova O, Kondratov RV. Circadian clock protein BMAL1 regulates cellular senescence in vivo. Cell Cycle. 2011; 10(23):4162–4169. [PubMed: 22101268]
24. Khapre RV, Kondratova AA, Patel S, Dubrovsky Y, Wrobel M, Antoch MP, Kondratov RV. BMAL1-dependent regulation of the mTOR signaling pathway delays aging. Aging (Albany NY). 2014 Jan; 6(1):48–57. [PubMed: 24481314]
25. Kondratov RV, Kondratova AA, Gorbacheva VY, Vykhovanets OV, Antoch MP. Early aging and age-related pathologies in mice deficient in BMAL1, the core component of the circadian clock. Genes Dev. 2006a; 20(14):1868–1873. [PubMed: 16847346]
26. Lin F, Chen Y, Li X, Zhao Q, Tan Z. Over-expression of circadian clock gene BMAL1 affects proliferation and canonical Wnt pathway in NIH-3T3 cells. Cell Biochem. Funct. 2013; 31(2): 166–172. [PubMed: 22961668]

27. Lipton JO, Yuan ED, Boyle LM, Ebrahimi-Fakhari D, Kwiatkowski E, Nathan A, Güttler T, Davis F, Asara JM, Sahin M. The circadian protein BMAL1 regulates translation in response to S6K1-mediated phosphorylation. Cell. 2015 May 21; 161(5):1138–1151. [PubMed: 25981667]

28. Maronde E, Schilling AF, Seitz S, Schinke T, Schmutz I, van der Horst G, Amling M, Albrecht U. The clock genes Period 2 and Cryptochrome 2 differentially balance bone formation. PLos One. 2010; 5(7):e11527. [PubMed: 20634945]

29. Maurel DB, Jaffre C, Rochefort GY, Aveline PC, Boisseau N, Uzbekov R, Gosset D, Pichon C, Fazzalari NL, Pallu S, Benhamou CL. Low bone accrual is associated with osteocyte apoptosis in alcohol-induced osteopenia. Bone. 2011 Sep; 49(3):543–552. [PubMed: 21689804]

30. McElderry JD, Zhao G, Khmaladze A, Franceschi RT, Morris MD. Tracking circadian rhythms of bone mineral deposition in murine calvarial organ cultures. J. Bone Miner. Res. 2013; 28(8):1846–1854. [PubMed: 23505073]

31. Meyer T, Kneissel M, Mariani J, Fournier B. In vitro and in vivo evidence for orphan nuclear receptor RORα function in bone metabolism. Proc. Natl. Acad. Sci. U S A. 2000; 96(16):9197–9202. [PubMed: 10900268]

32. O'Brien CA, Nakashima T, Takayanagi H. Osteocyte control of osteoclastogenesis. Bone. 2013 Jun; 54(2):258–263. [PubMed: 22939943]

33. Patel SA, Velingkaar NS, Kondratov RV. Transcriptional control of antioxidant defense by the circadian clock. Antioxid Redox Signal. 2014 Jun 20; 20(18):2997–3006. Epub 2014 Jan 3. [PubMed: 24111970]

34. Pignolo RJ, Suda RK, McMillan EA, Shen J, Lee Sh, Choi Y, Wright AC, Johnson FB. Defects in telomere maintenance molecules impair osteoblast differentiation and promote osteoporosis. Aging Cell. 2008; 7(1):23–31. [PubMed: 18028256]

35. Pritchard JJ. A cytological and histochemical study of bone and cartilage formation in the rat. J. Anat. 1952 Jul; 86(3):259–277. [PubMed: 12980877]

36. Pritchard, JJ. The osteoblast. In: Bourne, G., editor. The Biology and Physiology of Bone. 2nd. Amsterdam: Elsevier Publishing Company Inc; 1972. p. 21-43.

37. Quevedo I, Zuniga AM. Low bone mineral density in rotating-shift workers. J. Clin. Densitom. 2010 Oct-Dec;13(4):467–469. [PubMed: 21029978]

38. Reale ME, Webb IC, Wang X, Baltazar RM, Coolen LM, Lehman MN. The transcription factor Runx2 is under circadian control in the suprachiasmatic nucleus and functions in the control of rhythmic behavior. PLoS One. 2013; 8(1):e54317. [PubMed: 23372705]

39. Riddle RC, Clemens TL. Insulin, osteoblasts and energy metabolism: why bone counts calories. J. Clin. Invest. 2014; 124(4):1465–1467. [PubMed: 24642463]

40. Schaffler MB, Cheung WY, Majeska R, Kennedy O. Osteocytes: master orchestrators of bone. Calcif. Tissue Int. 2014 Jan; 94(1):5–24. Epub 2013 Sep 17. [PubMed: 24042263]

41. Soltanoff CS, Yang S, Chen W, Li YP. Signaling networks that control the lineage commitment and differentiation of bone cells. Crit. Rev. Eukaryot. Gene Expr. 2009; 19(1):1–46. [PubMed: 19191755]

42. Stanford CM, Jacobson PA, Eanes ED, Lembke LA, Midura RJ. Rapidly forming apatitic mineral in an osteoblastic cell line (UMR 106-01 BSP). J. Biol. Chem. 1995 Apr 21; 270(16):9420–9428. [PubMed: 7721867]

43. Takarada T, Kodama A, Hotta S, Mieda M, Shimba S, Hinoi E, Yoneda Y. Clock genes influence gene expression in growth plate and endochondral ossification in mice. J. Biol. Chem. 2012 Oct 19; 287(43):36081–36095. Epub 2012 Aug 30. [PubMed: 22936800]

44. Tatsumi S, Ishii K, Amizuka N, Li M, Kobayashi T, Kohno K, Ito M, Takeshita S, Ikeda K. Targeted ablation of osteocytes induces osteoporosis with defective mechanotransduction. Cell Metab. 2007 Jun; 5(6):464–475. [PubMed: 17550781]

45. Van der Linden JC, Days JS, Verhaar JA, Weinans H. Altered Tissue Properties induce changes in cancellous bone architecture in aging and diseases. J. Biomech. 2004 Mar; 37(3):367–374. [PubMed: 14757456]

46. Vogel H, Lim DS, Karsenty G, Finegold M, Hasty P. Deletion of Ku86 causes early onset of senescence in mice. Proc. Natl. Acad. Sci. U S A. 1999; 96(19):10770–10775. [PubMed: 10485901]

47. Wang A, Martin JA, Lembke LA, Midura RJ. Reversible suppression of in vitro biomineralization by activation of protein kinase A. J. Biol. Chem. 2000 Apr 14; 275(15):11082–11091. [PubMed: 10753913]

48. Zvonic S, Ptitsyn AA, Kilroy G, Wu X, Conrad SA, Scott LK, Guilak F, Pelled G, Gazit D, Gimble JM. Circadian oscillation in gene expression in murine calvarial bone. J. Bone Miner. Res. 2007; 22(3):357–365. [PubMed: 17144790]

Highlights

- The circadian clock regulates organismal bone physiology.
- A circadian clock deficient mouse model exhibits a low bone mass phenotype and what appears to be accelerated bone aging
- The circadian clock controls bone homeostasis, in part, by regulating mesenchymal stem cell osteoblastogenesis *in vivo* and *in vitro*.
- Extends findings on circadian clock control of bone homeostasis to show that BMAL1 deficiency causes a low bone mass phenotype.

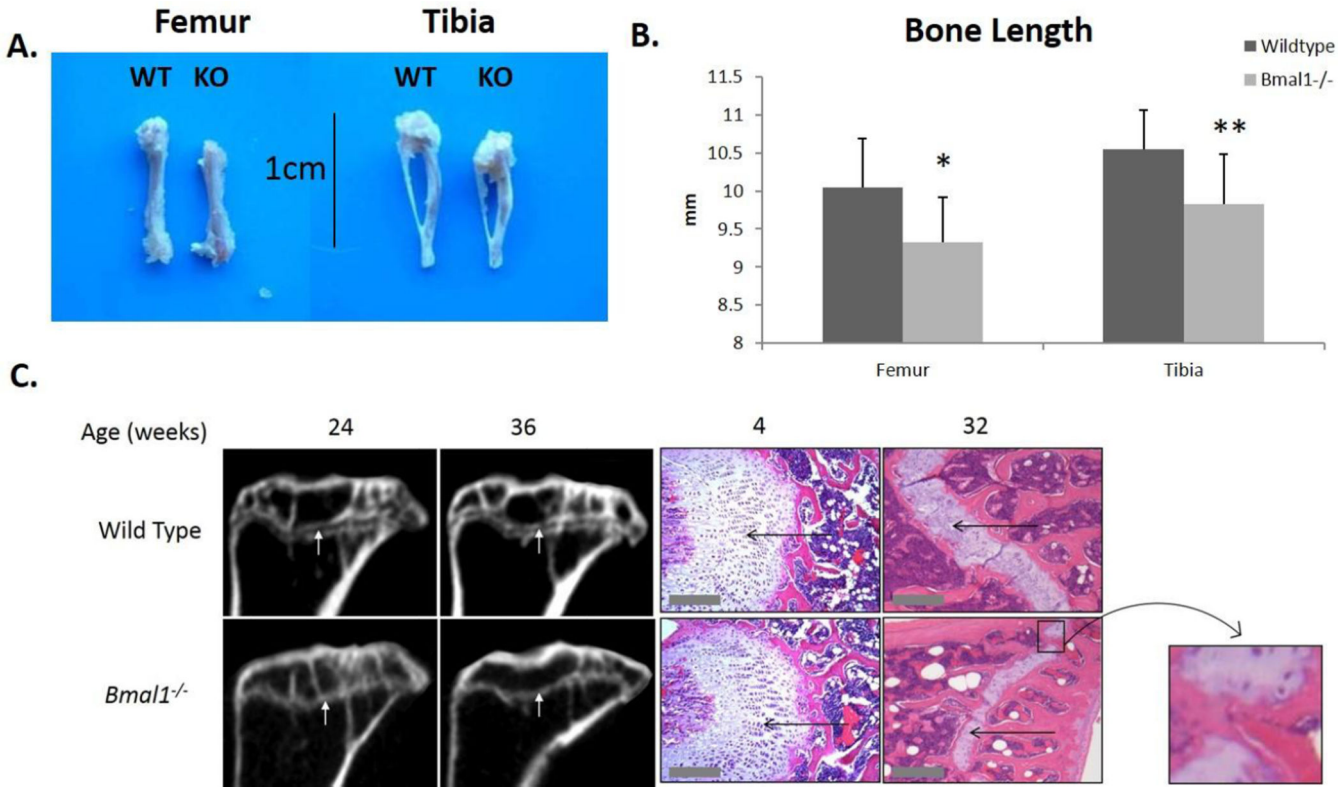

Figure 1. Bone bridging of the epiphyseal growth plate in mice deficient for BMAL1

A. Pictures of femora and tibiae from (left) wild type and (right) *Bmal1*$^{-/-}$ mice at 9 months of age. B. Micro-CT quantification of length of long bones. Dark bars represent wild type mice and light bars represent *Bmal1*$^{-/-}$ mice. * $p < 0.05$, ** $p < 0.01$. Femora: wild type n = 13, *Bmal1*$^{-/-}$ n = 12. Tibiae: wild type n = 14, *Bmal1*$^{-/-}$ n = 15. All mice are 9 months of age. C. Left: Micro-CT scan images of femur epiphyses from wild type and *Bmal1*$^{-/-}$ mice at 24 and 36 weeks of age. White arrows point to the epiphyseal plate/line. Right: H&E staining of the epiphyses of femora from wild type and *Bmal1*$^{-/-}$ mice at 4 weeks and 32 weeks of age. Thin black arrows point to the epiphyseal plate (white). Inset shows the closure of one bridge of the growth plate, where bone has fused. Scale bars: 200μm.

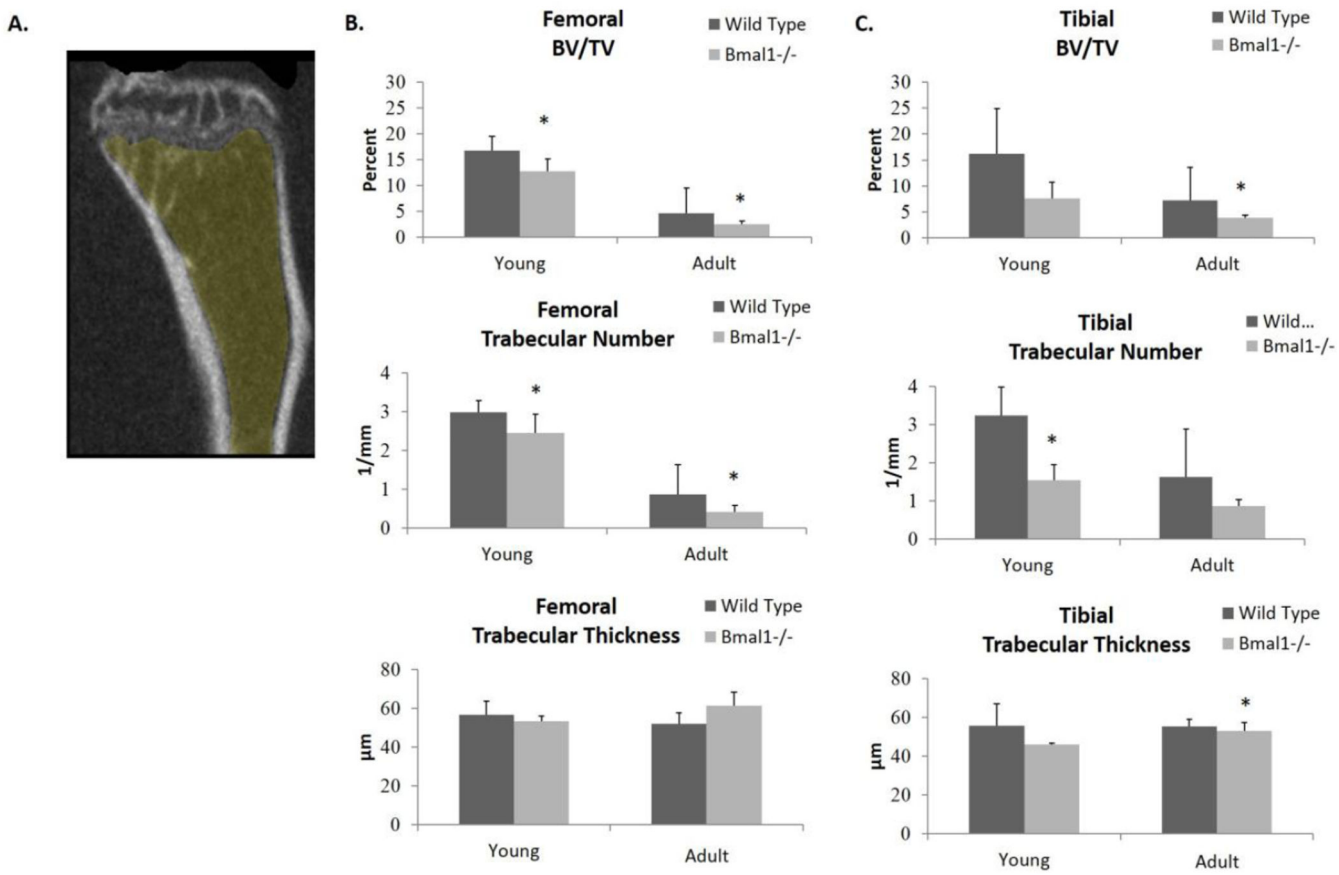

Figure 2. Micro-CT scan quantification of the trabecular bone architecture of femora and tibiae of wild type and *Bmal1*$^{-/-}$ mice

(A) Graphic representation of the region-of-interest (ROI) used for micro-CT scanning. All results presented are from the region-of-interest of femora and tibiae that are a distance of 0–25% from the distal femoral growth plate (GP) for femora and from the proximal tibial growth plate for tibiae. Shaded yellow region shows measurements taken excluding the primary spongiosa. Graphs show Micro-CT scans from (B) femora and (C) tibiae. Dark bars (Wild Type) represent wild type animals, and light bars (*Bmal1*$^{-/-}$) represent *Bmal1*$^{-/-}$ animals. Similar results were obtained from all ROIs. * indicates statistically significant difference between genotypes of the same age group (* $p < 0.05$, ** $p < 0.01$). BV/TV – Bone Volume Fraction. Young mice are 2 months of age, adult mice are 7–9 months of age. Sample size is minimum 3 animals per age and genotype.

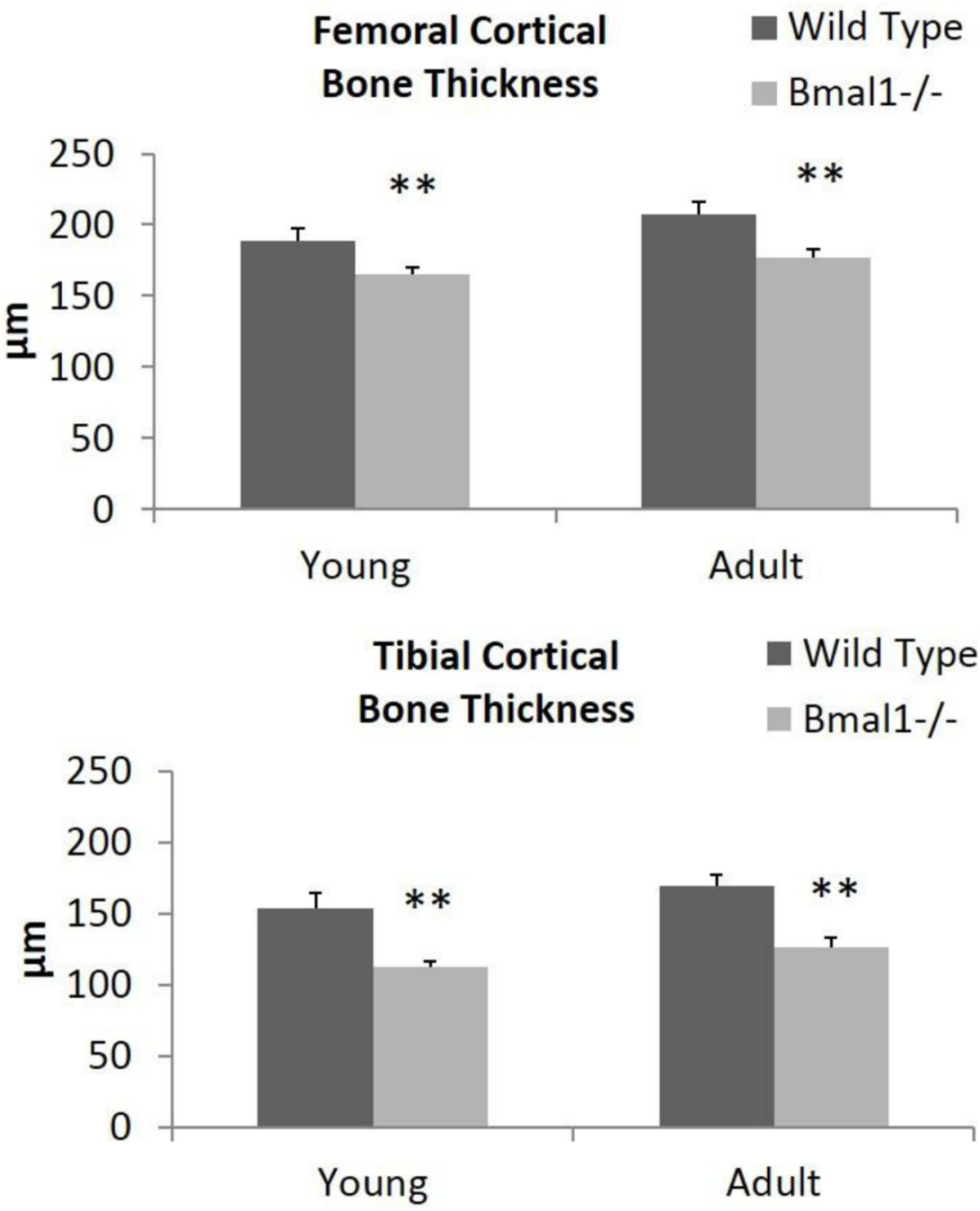

Figure 3. Micro-CT scan quantification of the cortical bone thickness of femora and tibiae of wild type and *Bmal1*$^{-/-}$ mice

All results presented are from the region-of-interest of femora and tibiae that are a distance of 0–25% from the distal femoral growth plate (femora) and from the proximal tibial growth plate (tibiae). Dark bars (Wild Type) represent wild type animals, light bars (*Bmal1*$^{-/-}$) represent *Bmal1*$^{-/-}$ animals. * $p < 0.05$, ** $p < 0.01$. Young mice are 2 months of age, adult mice are 7–9 months of age. Sample size is minimum 3 animals per age and genotype.

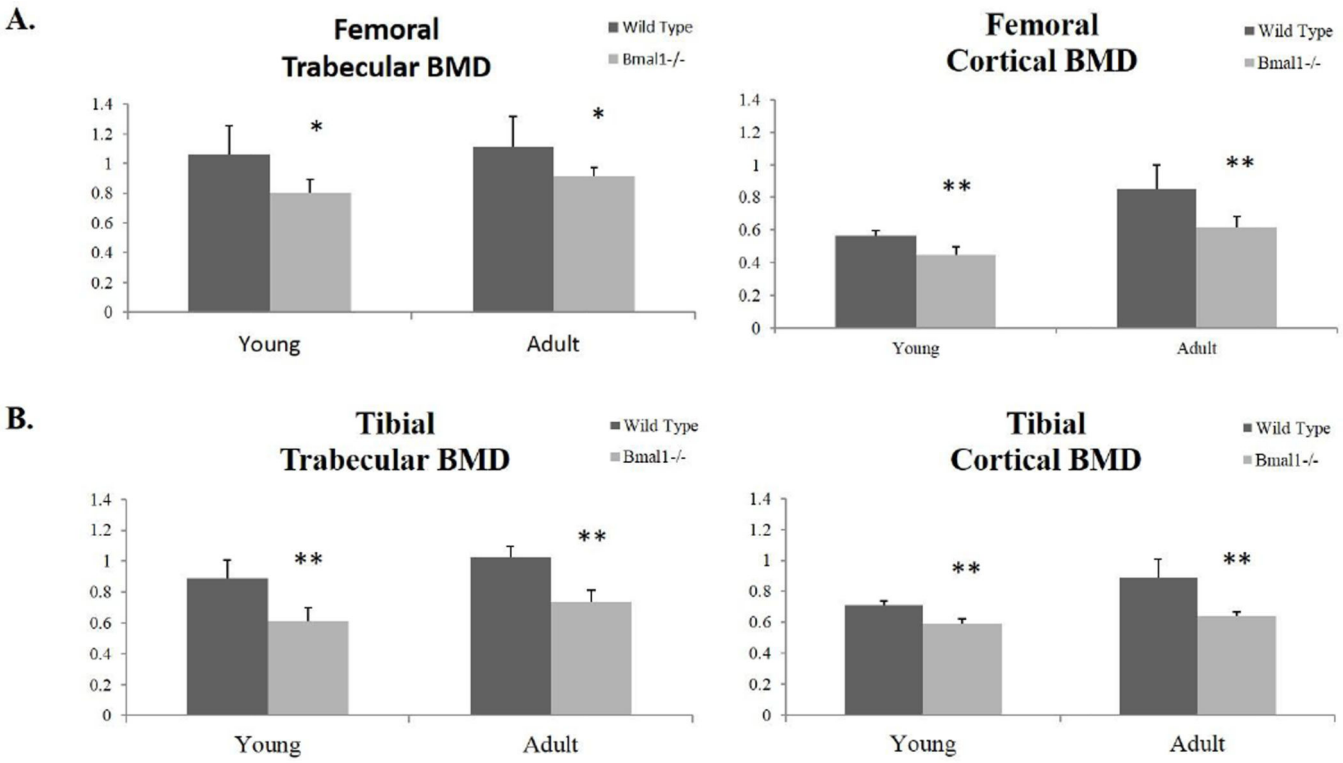

Figure 4. Micro-CT scan quantification of the bone mineral density (BMD) of (A) femora and (B) tibiae of wild type and *Bmal1*$^{-/-}$ mice

All results presented are from the region-of-interest of femora and tibiae that are a distance of 0–25% from the distal femoral growth plate (femora) and from the proximal tibial growth plate (tibiae). Dark bars represent wild type animals and light bars (*Bmal1*$^{-/-}$) represent BMAL1 deficient animals. * indicates statistically significant difference between genotypes of the same age group (* $p < 0.05$, ** $p < 0.01$). Young mice are 2 months of age, adult mice are 7–9 months of age. Sample size is minimum 3 animals per age and genotype.

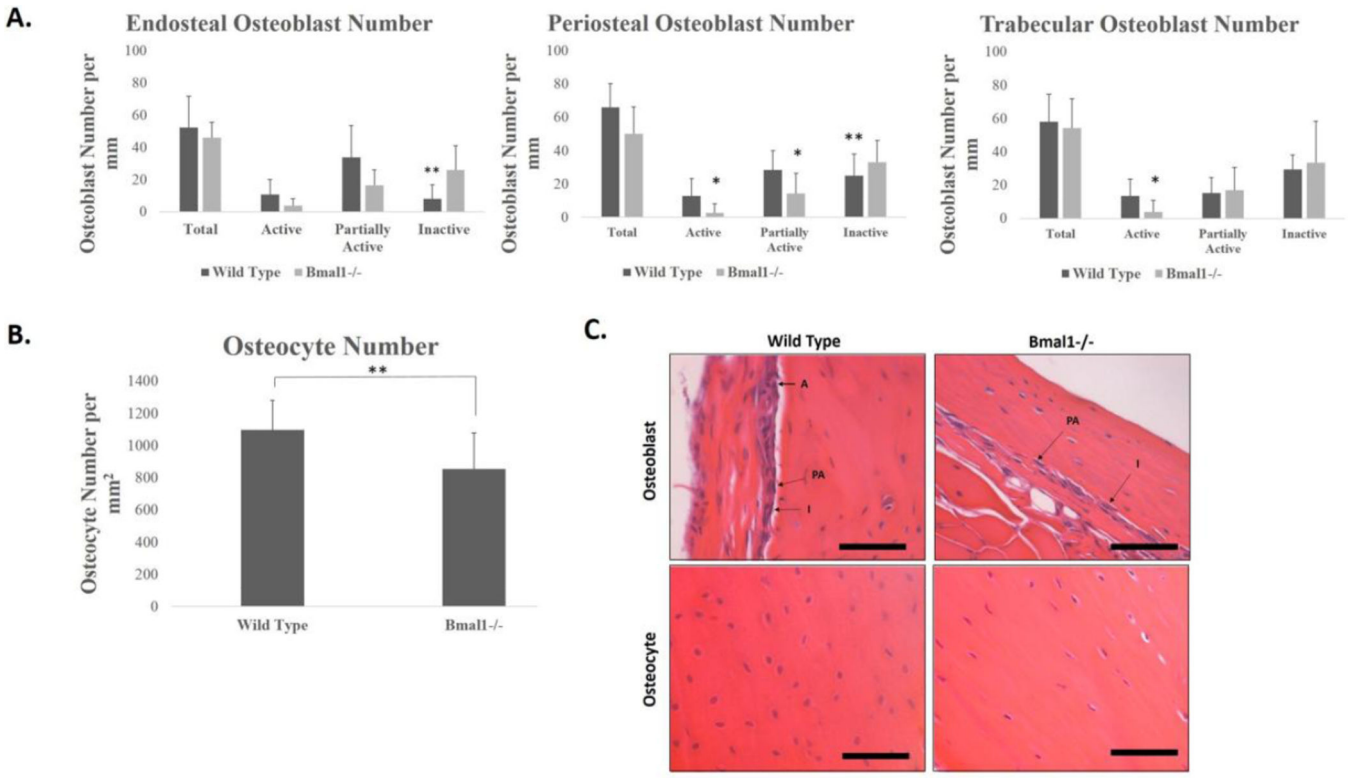

Figure 5. Reduced osteoblast and osteocyte number in *Bmal1*$^{-/-}$ mice

A. Number of osteoblasts per mm on the cortical endosteum, periosteum and trabecular endosteum per mm of bone surface in 6–7 month old wild type (dark bars) and 5–6 month old *Bmal1*$^{-/-}$ (light bars) mice. n = 3 mice for each genotype. (* $p < 0.05$, ** $p < 0.01$). B. Number of osteocytes per mm^2 of bone area in 6–7 month old wild type and 5–6 month old *Bmal1*$^{-/-}$ mice. ** $p < 10^{-13}$. n = 3 mice per genotype. C. Representative pictures of periosteal osteoblasts in wild type (upper left panel) and *Bmal1*$^{-/-}$ (upper right panel) femora. Arrows point to osteoblasts that are either active (A), partially active (PA) or inactive (I), as determined by the aspect ratio described in materials and methods. Lower panels show representative images of osteocytes from wild type (left) and *Bmal1*$^{-/-}$ (right) osteocytes. Scale bars = 50 μm.

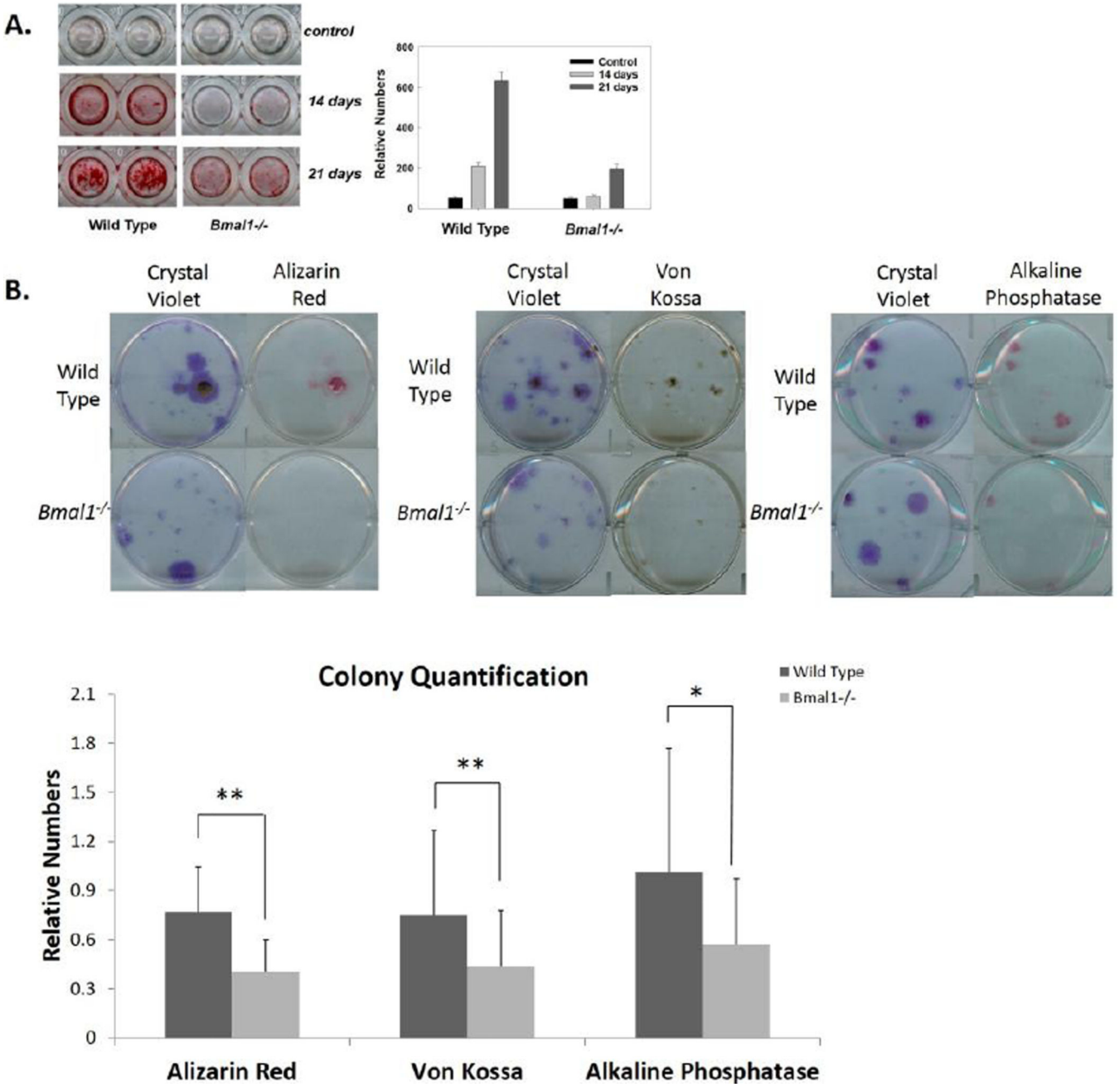

Figure 6. Impairment of Osteoblast Differentiation in *Bmal1*$^{-/-}$ Mice

A. Left: Alizarin red staining (ARS) of wild type and *Bmal1*$^{-/-}$ MSCs at 0, 14 and 21 days of culture in differentiation media. Cells were cultured for 3 passages before being plated into 96 well plates. Right: quantification of ARS in these cultures. *Bmal1*$^{-/-}$ MSCs show a delay in the onset of mineralization and a reduced intensity of staining. B. ARS, Von Kossa (VK), Alkaline Phosphatase (ALP), and Crystal Violet (CV) staining of MSCs. Isolated primary cells were directly plated into 6 well plates and induced to differentiation for 18 days. After staining for ARS, VK and ALP, the same plate was stained for CV to examine the total number of colonies present. Top: WT cells show a higher number of colonies that

stain positive and a stronger intensity of staining for ARS, VK, ALP and CV staining. Bottom: quantification of colony number. Colonies that stained positively for each stain was counted and normalized to the total number of colonies present as measured by CV staining. Data shows mean ± standard deviation for 20 replicates. Dark bars represent wild type (WT) colonies and light bars represent *Bmal1*$^{-/-}$ colonies. There is a significant decrease in the number of *Bmal1*$^{-/-}$ colonies that stained positive for ARS, VK and ALP. * $p < 0.05$, ** $p < 0.01$.